Supporting Information for "Seasonality and Buoyancy Suppression of Turbulence in the Bay of Bengal"

Ritabrata Thakur [1], Emily L. Shroyer [2], Rama Govindarajan[1], J. Thomas Farrar[3], Robert A. Weller[3], and James N. Moum[2]

[1]International Centre for Theoretical Sciences, Tata Institute of Fundamental Research, Bengaluru, Karnataka, India

[2]College of Earth, Ocean, and Atmospheric Sciences, Oregon State University, Corvallis, Oregon, USA

[3]Woods Hole Oceanographic Institution, Woods Hole, Massachusetts, USA

corresponding author - ritabrata.thakur@icts.res.in

Contents of this file

1. Text S1 to S3
2. Figures S1 to S7

Introduction This supporting information has section S1 detailing χpod data averaging, section S2 on how to access the dataset, section S3 on wavelet transforms, and figures (S1 - S7) in support of the main manuscript.

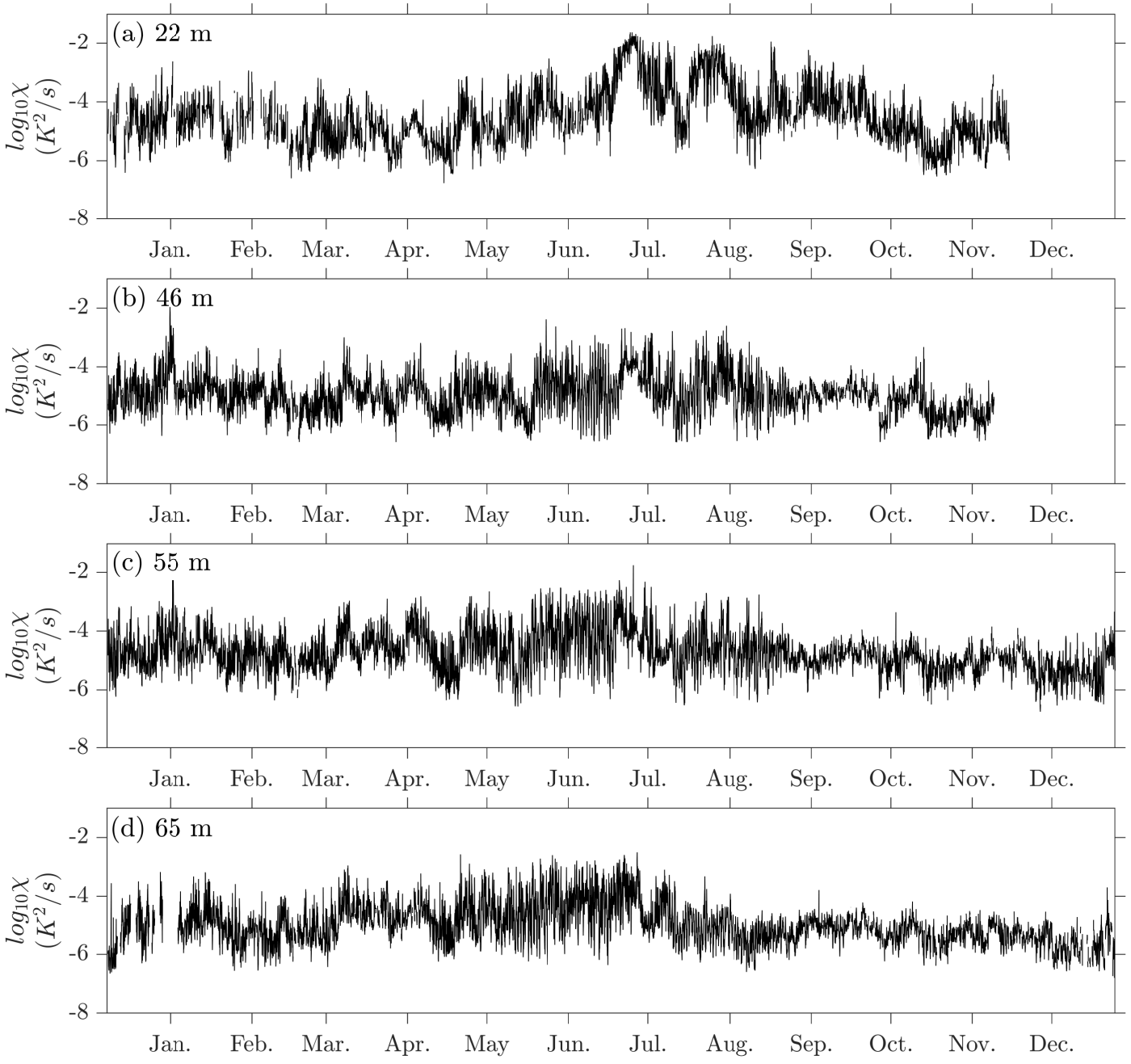

Figure S1. Hourly averages of decay rate of temperature variance (χ) as measured with the four χpods at (**a**) 22 m, (**b**) 46 m, (**c**) 55 m, and (**d**) 65 m.

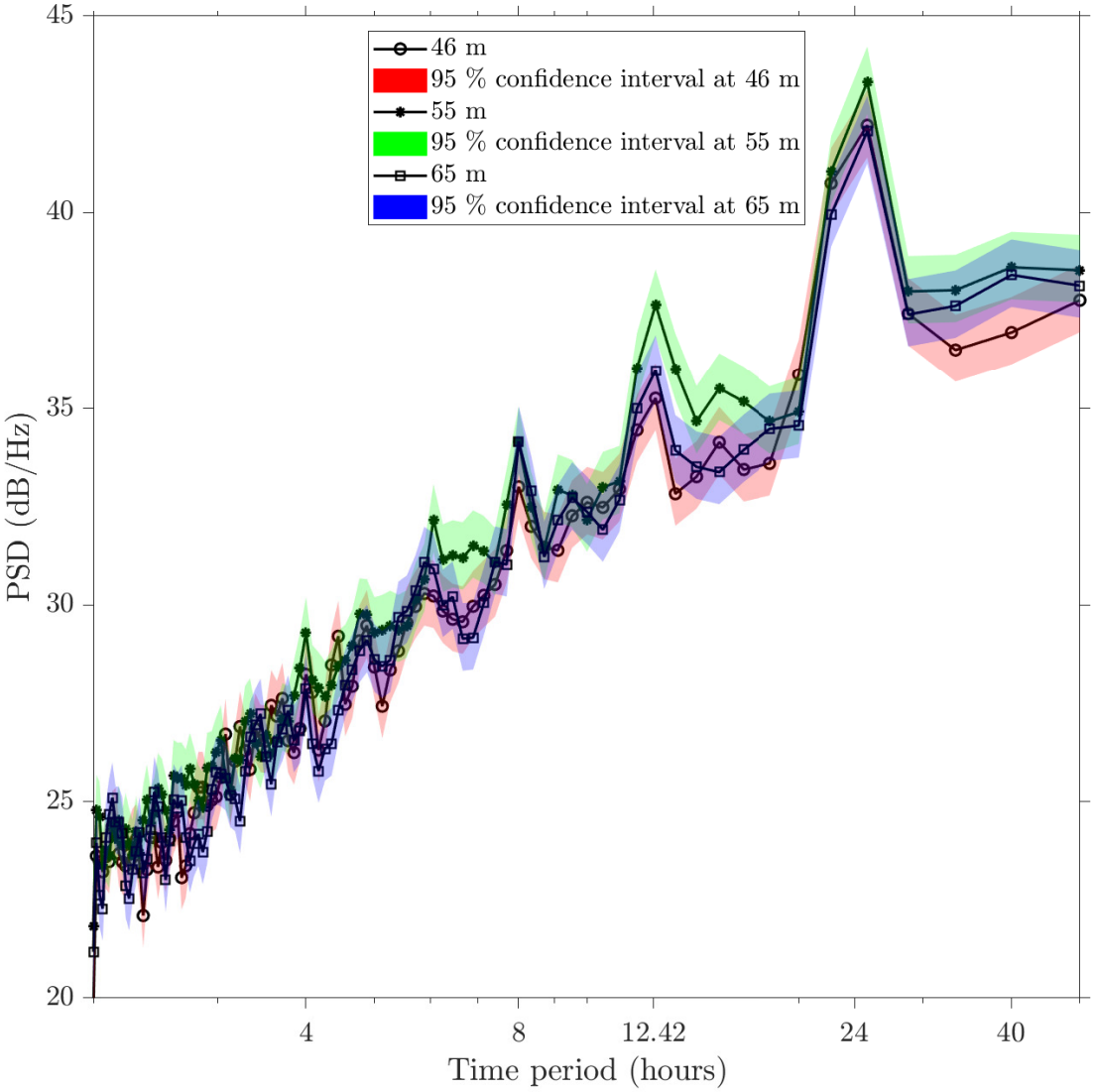

Figure S2. Power spectral densities of hourly-averaged $\boldsymbol{log_{10}K_t}$ at 46 m, 55 m, and 65 m for the whole period of deployment from December 2014 to December 2015 showing diurnal and shorter time period variability. The red, green, and blue shadings denote the 95% confidence intervals for 46, 55, and 65 m respectively. The inertial period at 18° N is $\sim$ 39 hours.

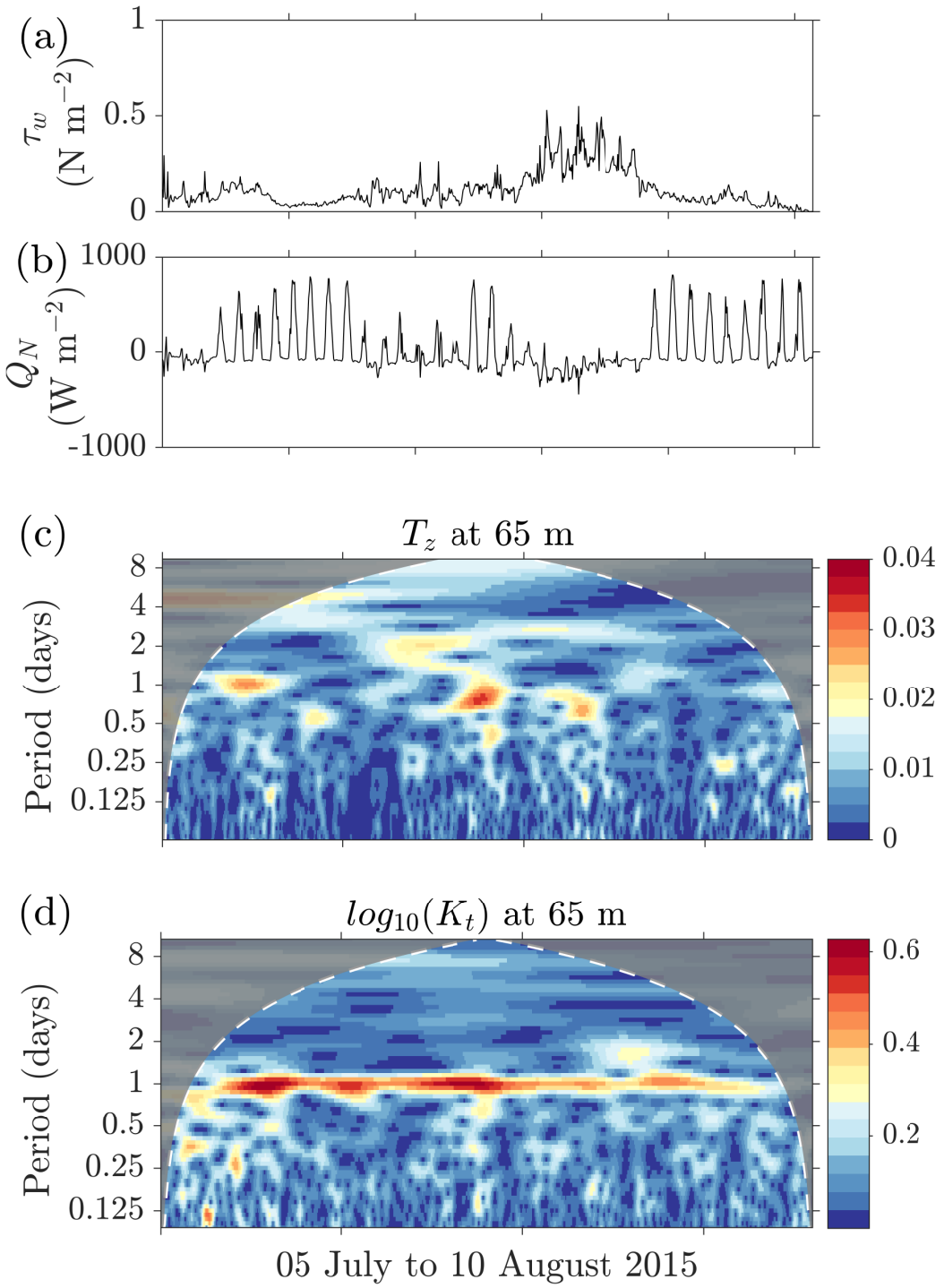

Figure S3. Hourly averages of (**a**) wind stress τ_w, (**a**) net atmospheric heat flux Q_N. Wavelet transforms of (**c**) T_z at 65 m and (**d**) $log_{10}K_t$ at 65 m for the period of 05 July to 10 August.

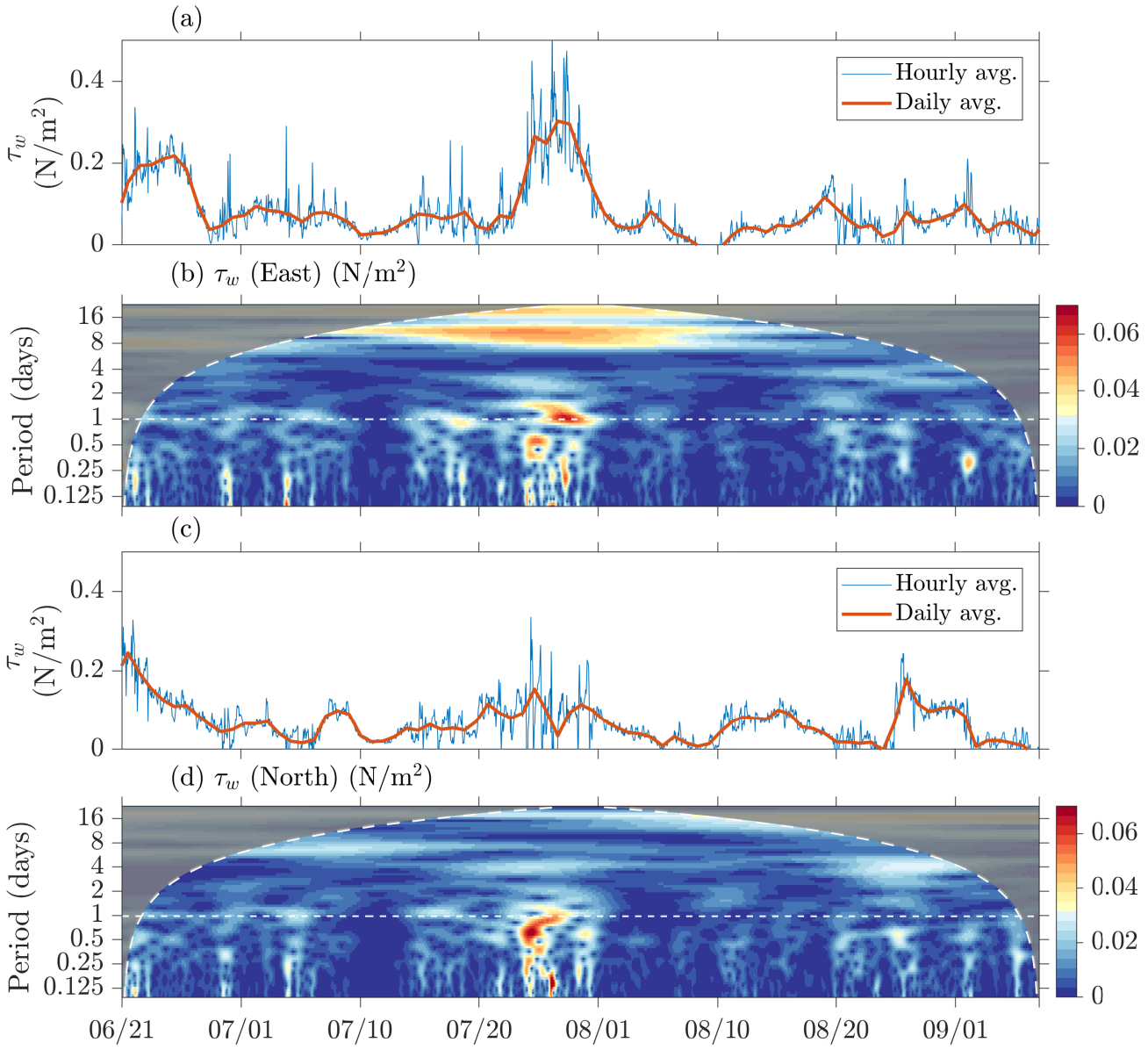

Figure S4. Hourly and daily averages of wind stress $\boldsymbol{\tau_w}$ in (**a**) East and (**c**) North directions for ∼2.5 months period within the SW monsoon. (Note that the narrowband and persistent diurnal signal in diffusivity at 65 m is seen from 05 July to 10 August.) Wavelet transforms of hourly-averaged $\boldsymbol{\tau_w}$ in (**b**) East and (**d**) North directions for the same time period. The white dotted lines in (**b**) and (**d**) mark the diurnal frequency.

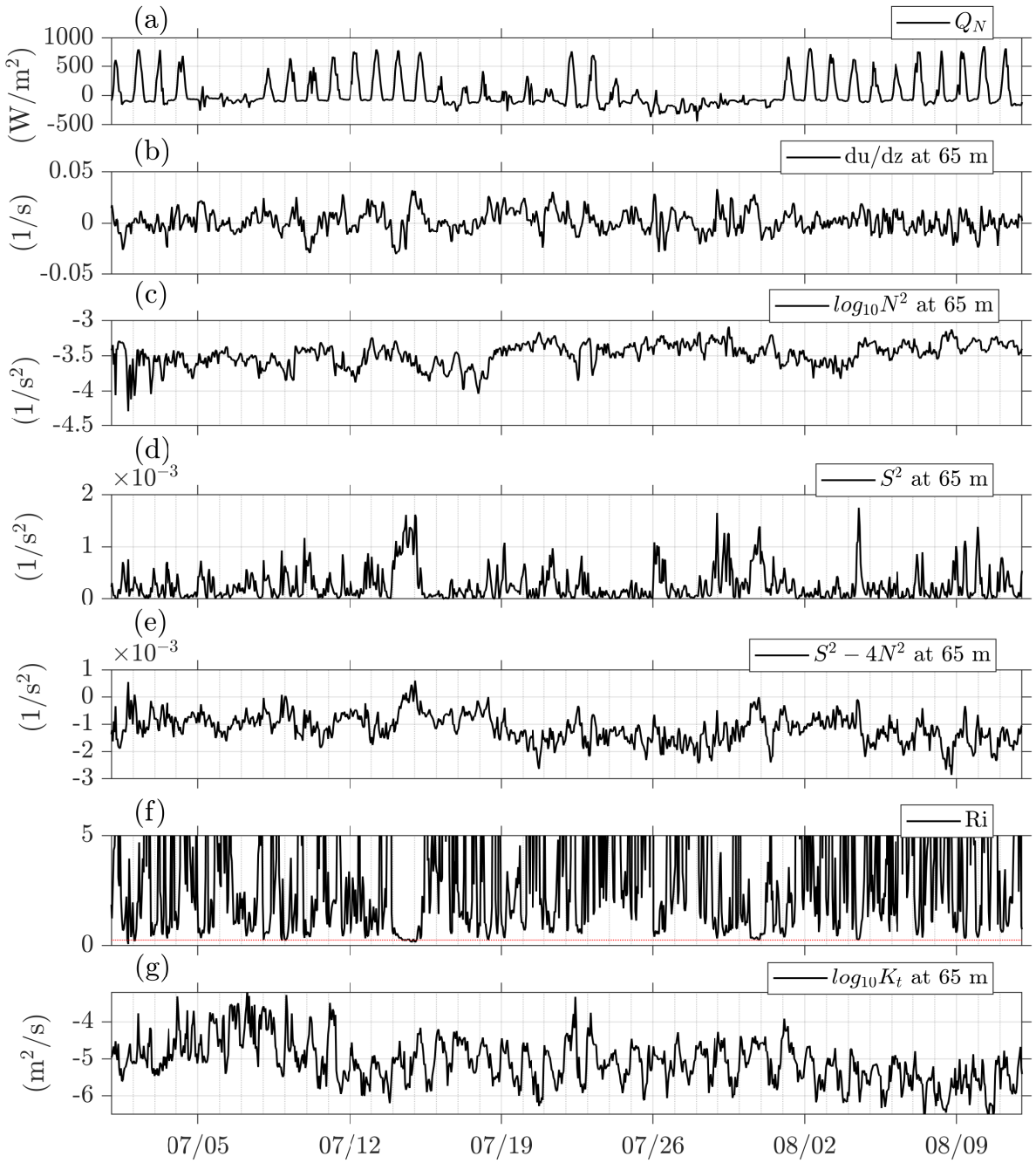

Figure S5. Hourly averages of (**a**) net atmospheric heat flux Q_N, (**b**) eastward shear at 65 m (The ADCP bins are 2 m apart in depth (z)), (**c**) Brunt-Väisälä frequency $log_{10}N^2$, (**d**) square of the total shear ($S^2 = (du/dz)^2 + (dv/dz)^2$) at 65 m, (**e**) S^2- $4N^2$ at 65 m, (**f**) Richardson number ($Ri = N^2/S^2$) at 65 m (red dotted line is the 1/4 value), and (**g**) diffusivity $log_{10}K_t$ at 65 m.

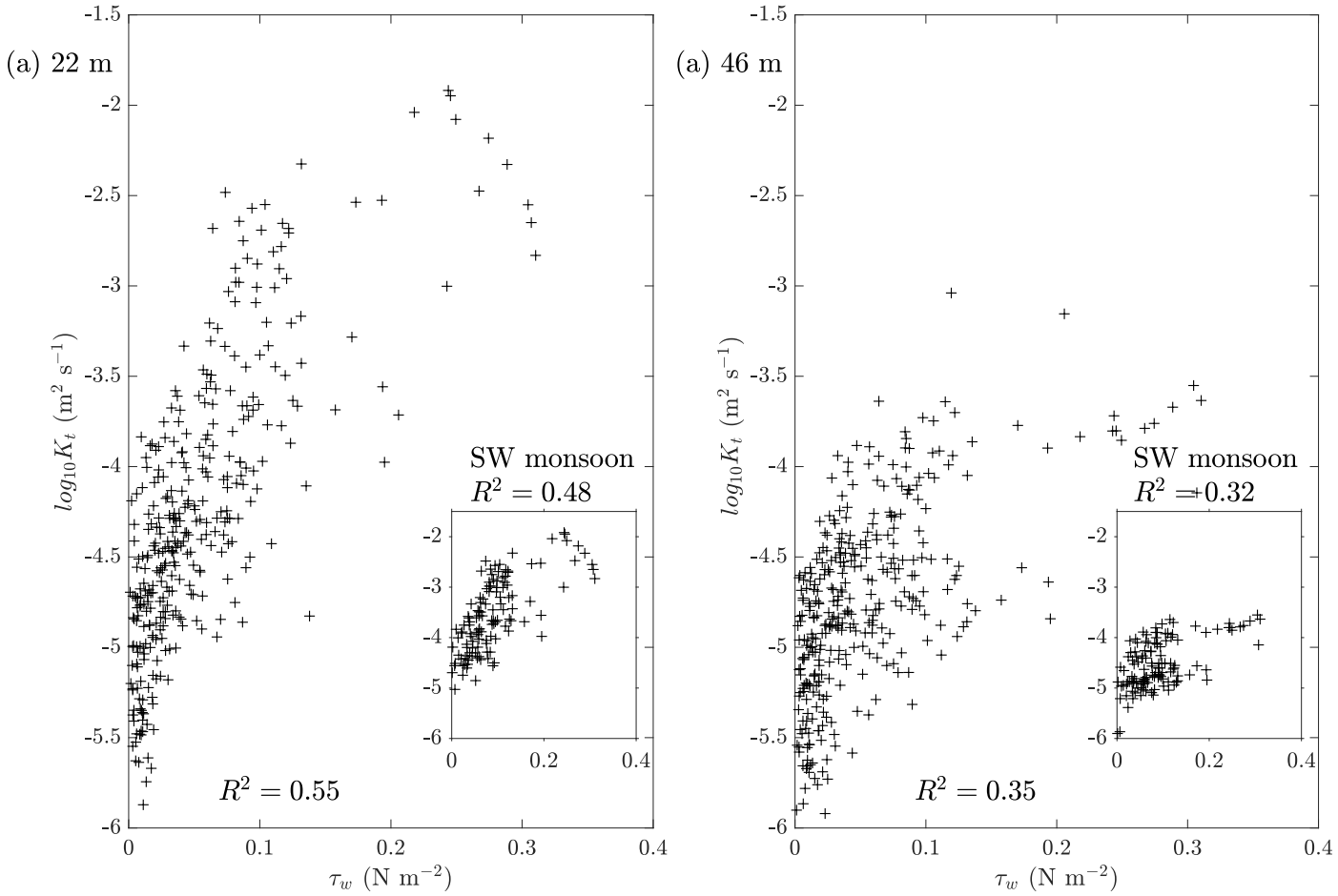

Figure S6. Correlations of daily averaged wind stress $\boldsymbol{\tau_w}$ and $\boldsymbol{log_{10}K_t}$ at (**a**) 22 m and (**b**) 46 m. Insets in (**a**) and (**b**) show correlations during the SW monsoon for the respective depths.

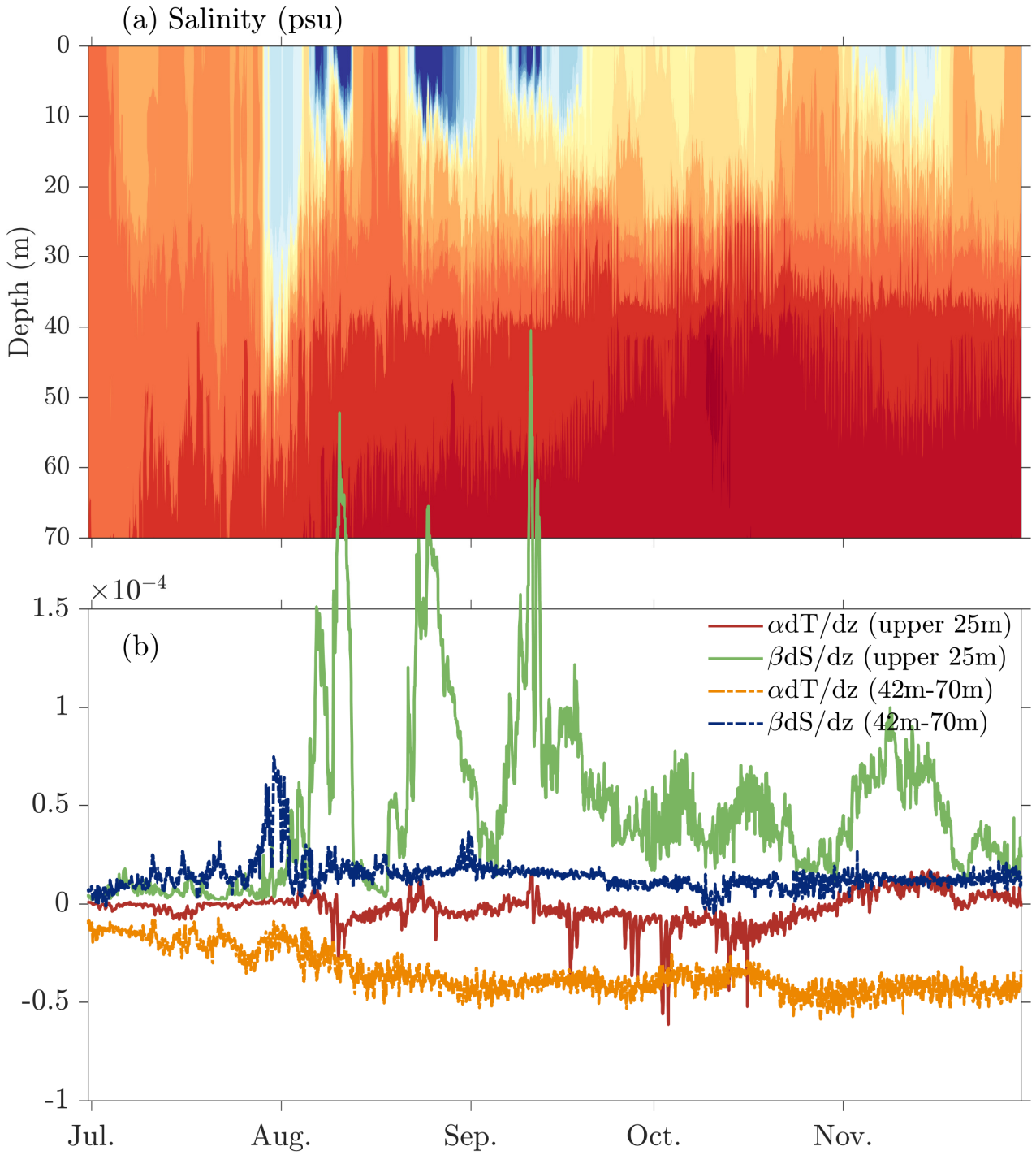

Figure S7. (**a**) Salinity and (**b**) relative contribution of salinity and temperature to density.

1. S1: χpod data averaging

The temperature variance decay rate is estimated directly from the χpod measurements. χ is also the integral of the power spectral density of the horizontal temperature gradient, ψ_{T_x},

$$\chi = 6\mathcal{D}\int_0^\infty \psi_{T_x}(k)dk \tag{1}$$

where $\mathcal{D}$ is the molecular diffusivity of heat, and the isotropy of temperature gradients is assumed.

Thermistors on χpods allow us to resolve turbulence in the viscous-convective sub-range of the Batchelor spectrum. Temperature gradient spectra (ψ_{T_x}) are calculated on 1-second sections, thus outside the surface wave band ($\sim$ 4-20 s). Fitting over a short time range also lends confidence to the assumption that turbulence in the period is stationary. Mean temperature and salinity (from CTDs) was sampled more slowly with effectively 10 minute-resolution so that surface wave contributions are averaged out of these data. We use a 10-minute average χ from 1-second individual estimates to derive 10-minute estimates of diffusivity (K_t).

The iterative algorithm used to calculate χ uses a constant mixing efficiency (Γ) of 0.2. Moum & Nash, 2009 showed that 1-s estimates of χ could vary by about 30% when Γ varies in the range of 0.1-0.35. For speeds < 0.7 m/s (appropriate to our observations) and during high ϵ periods, there could be a 30% change in the estimates of χ in the lowest Γ considered (0.1).

2. S2: Accessing the dataset

WHOI surface meteorology and air-sea flux data are available in *Upper Ocean Processes Group, 2016*. Upper-ocean temperature, salinity, turbulence, and current data are available in *Upper Ocean Data, 2018*.

3. S3: Wavelet Transforms

By "wavelet transform", we mean continuous one-dimensional wavelet transform of a signal using one of the many available analytic wavelets. These analytic wavelets are wavelike oscillatory functions localized both in time and frequency space. These functions are rapidly decaying in time and have a zero mean. Wavelet transforms allow us to analyze oscillatory signals ($f(t)$) that vary both in time and frequency by extracting the amplitude of convolutions with analytic wavelets [Lilly & Olhede, 2010, 2012; Olhede & Walden, 2002]. The analytic wavelets used in our study are the generalized Morse wavelets.

4. References

Lilly, J. M., & Olhede, S. C. (2010). On the analytic wavelet transform. *IEEE Transactions on Information Theory, 56(8)*, 4135-4156.

Lilly, J. M., & Olhede, S. C. (2012). Generalized Morse wavelets as a superfamily of analytic wavelets. *IEEE Transactions on Signal Processing, 60 (11)*, 6036–6041.

Moum, J. N., & Nash, J. D. (2009). Mixing measurements on an equatorial ocean mooring. *Journal of Atmospheric and Oceanic Technology, 26 (2), 317–336.*

Olhede, S. C., & Walden, A. T. (2002). Generalized Morse wavelets. *IEEE Transactions on Signal Processing, 50 (11)*, 2661–2670.

Upper Ocean Processes Group. (2016). http://uop.whoi.edu/projects/Bengal/.

Upper Ocean Data. (2018). https://doi.org/10.6084/m9.figshare.7416440.